



Dynamic instability visualization of a rubber/glass interface

Deleau Fabrice ^{a,b}, Mazuyer Denis ^a,
Perret-Liaudet Joël ^a, Le Bot Alain ^a,
Rigaud Emmanuel ^a, Koenen Alain ^b.

^a Laboratoire de Tribologie et dynamique des Systèmes, UMR 5513,
Ecole Centrale de Lyon, 36 avenue Guy de Collongue, 69131 Ecully, France
^b Valeo Système d'Essuyage, 8 rue Louis Normand 78321 La Verrière, France

ABSTRACT

The wiping of a windshield is achieved by the reciprocating motion of a blade. This function is performed by a rubber/glass contact of micrometric dimension. Under certain wetting conditions, wear, clean of the glass, a very annoying noise is perceptible within the car passenger compartment. Comparable systems are poorly studied and the physical phenomena present at the interface require a better understanding to improve the quality of this product.

This article proposes a qualitative study of contact vibrations. The interface consists of a rough elastomer sliding on a smooth glass surface in total wetting conditions. The observation of this multi-contact area is realized through a modified ElastoHydroDynamics tribometer. This device put in contact an elastomer fixed part on a rotating glass disk, the loading and kinematics of are perfectly controlled. Interferometric technique combined with an ultra fast recording camera permit to measure the contact area and the blade movement. This original experimental approach is based on a visual system and a set of dynamical sensors.

The contact observation and the acoustic emission characteristics permit to say that the radiated noise was initiated by the friction fluctuation. The vibration is measured in the sliding direction leads to the conclusion that the instabilities are well-type stick slip. This study validates the fact that the auto generated vibration of the elastomer/glass contact is a stick slip problem and generates squealing noise. Profile dimensions define the rubber contact stiffness. The materials determine the friction coefficient and the contact area density.

1 INTRODUCTION

1.1 Background

Windscreen wiping consists of the reciprocating motion of a rubber blade on a more or less wetted glass in order to remove water from the glass surface [1]. Despite the importance between windcreens wiping efficiency on driver safety in terms of visibility improvement and noise emission reduction, the squealing occurrences is unclear. The analysis of small contact between rubber and glass (a few tens of square millimeters), considered with a large scale of sliding velocity in fully wetting conditions, requires a better understanding of the contact frictional response and its stability.

^a Email address: fabrice.deleau@gmail.com

^b Email address: alain.koenen@valeo.com

1.2 Condition of vibration apparition

During the sliding of an elastomer block on an unspecified substrate, rapid processes usually occur, contact vibrations are observed at the sliding interface. These phenomena can take place at various length scales, starting at molecular distances. The most well known instability for rubber is the so-called Schallamach waves [2]. These instabilities have been observed with a glass lens slider pressed on a smooth flat rubber substrate at a $100 \mu\text{m}\cdot\text{s}^{-1}$ sliding velocity [3]. Schallamach waves are considered as “tunnels” of air that provide relative displacement between the slider and the substrate rather than the instantaneous interfacial failure involved with stick slip. To form these structures, the adhesive forces at the interface must be strong enough to pin the interface in the rear of the contact area creating a zone of tension, while shearing the interface causes a zone of compression in front of the contact area.

On the larger scale, instabilities usually appear when the kinetic friction coefficient decreases with increasing sliding velocity [4] [5]. These vibrations have been observed with a simple mass spring system performed over a wide range of relevant control parameters, namely, the imposed sliding velocity at which the "free" end of the pulling spring is being driven, the spring stiffness and the slider mass [4]. Stick slip motion or sprag-slip phenomenon [7], succession of stick and slip phase, may occur on many different length (the sliding jump reach $2 \mu\text{m}$ to 10mm) and time scales, the instability frequency can evolve between 1 to 5000 Hz [8].

In order to analyze the wiper blade dynamical behavior, previous works are based on the modeling of a real wiping device to take into account the global structure stiffness [9] [10] [11]. All these experiments do not observed at the local scale what happened whereas Schallamach waves could appear at micrometer length scale [2].

1.3 Friction mechanism

The elastomer friction does not follow the classic friction law due to its viscoelastic aspect [2] and its important adhesive component [12] [13]. Two main factors contribute to the friction between surfaces in relative motion. The first and usually the most important is the adhesion force, which occurs in the region of the real contact area. A second term may be described as a deformation component [12]. If no coupling exists between these two factors, it is possible to calculate, at constant normal load, a friction coefficient, μ , such as follows (1):

$$\mu = \mu_{Adhesive} + \mu_{Hysteresis} \quad (1)\square$$

Thus, the classic laws of friction as they evolved from the early work of da Vinci, Amontons and Coulomb may be summarized as follows [15]:

- The friction force is proportional to the load.
- The friction coefficient is independent of the apparent contact area.
- The static coefficient is larger than the kinetic one.
- The friction coefficient is independent of the sliding velocity.

It is now established, that only the first law is correct, except at high pressures when the real contact area approaches the apparent contact area. In dry environment, according to Schallamach [2] and Barquins [16] the friction force is velocity dependent and takes a maximum value around a few centimeters per second. The phenomenon interpretation differs according to these authors:

- A succession of adhesion and ruptures called waves of Schallamach [2] are prevalent at low velocity. A critical velocity promotes adhesion friction interaction so a maximum friction is observed.
- The second theory concludes that the friction is proportional to the viscoelastic aspect of the rubber and the damping factor (tangent modulus, $\tan \delta$) and it is inversely proportional to material hardness.

However, these authors claim that elastomer sliding induces a succession of creation and rupture of connections and confirm the friction coefficient velocity dependence. The relation between the tangent modulus, frequency and temperature has been developed by William-Landel-Ferry [17]. The WLF transformation shows that the sliding rubber friction at various velocities and temperatures can be entirely described by a simple main curve and the glass transition temperature, T_g , of the elastomer part [3] [18].

The influence on a squeeze film in the contact perturbs the friction mechanism. The friction coefficient decreases with the sliding velocity due to the lubricating effect [19] [21] or due to the smoothing effect of the liquid [22]. The water may fill the rubber cavities and permits to obtain a roughness decrease.

1.4 Goal of this study

This paper analyzes the behavior of the rubber/glass contact when unpleasant sound, like squealing, is emitted to characterize the vibration phenomenon and to define the noise controlling parameters. Most of the time, squealing appears on wiping device in fully wetting conditions so the contact instabilities are observed in these conditions and all these aspects are the subject of detailed attention.

2 EXPERIMENTAL SETUP

2.1 The IRIS Tribometer

The instability phenomenon has been evaluated using the IRIS tribometer which is derived from an ElastoHydroDynamical test rig developed in our laboratory [20]. This system realized a contact between a steel ball and a glass disk. All conditions like the normal load, the kinematics, the lubricant feed are controlled. It allows the study of lubricated phenomenon by the simultaneously measurement of the friction coefficient and the visualization of the contact area.

A schematic view of the modified system is given in Figure 1 and its main characteristics are summarized in Table 1. The specificity of this tribometer is the simultaneous dynamical measurement of solicitation and the visualization of the contact in controlled kinematics' conditions. The contact is realized between a fixed rubber specimen and a silica disc ($\Phi = 90$ mm). The gap between antagonistic asperities can be measured using interferometric technique [23]. The kinematics of this contact is controlled by the rotational motion of the disc which is obtained using a brushless motor. The velocity resolution is 1/100000 steps per revolution per second. Thus, numerous contact kinematics can be generated within a range of sliding velocity, from $100 \mu\text{m}\cdot\text{s}^{-1}$ to $2 \text{m}\cdot\text{s}^{-1}$. The applied normal load can be varied to a maximum of 20 N and it is estimated with the sample displacement. A torque sensor, located between the disc and the brushless motor, allows us to measure the friction force during each test. Visualization, friction force measurements and all sensor signals are simultaneously acquired by a personal computer. Dynamical applied forces on the elastomer sample are measured through a 3D piezo electric force transducer. The vibration characteristics like speed and displacement are recorded with a vibrometer pointed on the elastomer lip.

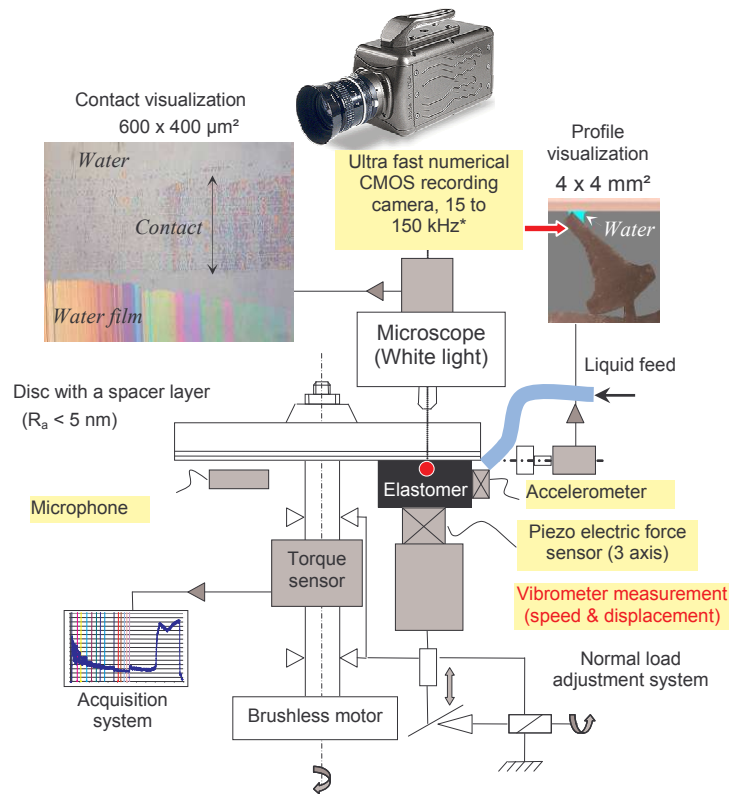


Figure 1: Schematic view of the IRIS Tribometer

Table 1: Performance of the IRIS Tribometer

Parameters	Range
Sliding velocity, V_g	$100 \mu\text{m}\cdot\text{s}^{-1}$ to $2 \text{m}\cdot\text{s}^{-1}$
Normal load F_z	0 to 20 N (resolution 0.1N)
Friction torque	0 to 2 Nm (resolution 10^{-4} Nm)

A high-speed numerical CMOS recording camera is used to visualize the contact motion. In the same time, the sound emission is recorded through a $\frac{1}{2}$ inch microphone. The tribometer is placed in a chamber covered inside by a highly absorbed material in order to reduce the background noise (Chamber volume is 1m^3). The maximum acquisition frequency is 40 kHz for each five-acquisition ways (3D forces, accelerometer, and microphone) and the image acquisition is limited to 15 kHz.

2.2 Materials in contact

In order to simulate the windscreen wiper/glass contact, roll-shaped elastomer specimens have been supplied by Valeo Wiper System. Different sample geometries have been studied (see Figure 2), real profiles and simplified geometries: the sample length is 30 mm and the radius of curvature of the surface is 0.5 mm. The elastic mechanical properties of these compound elastomers have been determined by Valeo with traction tests in stabilized mode and identified a Mooney Rivlin

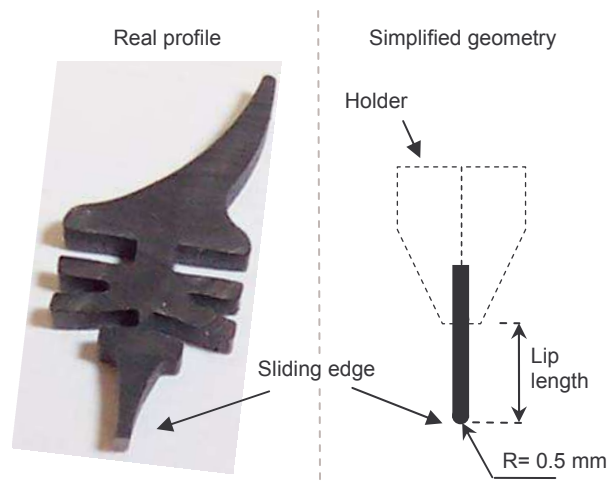


Figure 2: Slider geometries

extrapolation with two parameters: the Young's modulus is approximately 6 MPa at 20°C with a relative elongation less than 40%. Since the elastomer is considered as an incompressible material, the Poisson's ratio is about 0.5. Carbon blacks are used to reinforce these rubber samples. Their glass transition temperature is -62°C. Sample roughness has been measured using optical interferometry: the surface mean roughness SPA is 1 μm . Scanning Electron Microscopy has been used to observe and check the surface homogeneity.

The contact is realized between the elastomer specimens and a silica disc. The latter is covered with a 10 nm thick semi-reflective chromium layer and with an additive 200 nm thick spacer layer. The average roughness of the glass surface is less than 5 nm and is considered as smooth, compared to the elastomer. The following Table 2 presents the properties of the materials in contact.

Table 2: Mechanical material properties

Parameters	value	Parameters	value
E_{Glass}	106 GPa	E_{Rubber}	6 MPa
ν_{Glass}	0.17	ν_{Rubber}	0.5

Two special attentions are given to the tribometer: one to the position of the disk on its rotation shaft and another to the elastomer specimen position. The contact edge must be parallel to the glass surface in order to give a homogenous contact along the total edge.

2.3 The contact area measurement

The chromium layer deposited on the glass surface reflects half part of the white light emitted by the microscope and the second part is reflected by the rubber asperities. This beam shift creates interferometric fringes acquired with a numerical camera. First, the film thickness color correspondence is gauged with a known configuration and the calibrate silica disc: an ElastoHydroDynamical contact is established between a steel ball and the previously described silica disc. Visualization of the contact formed between the two solids allows a precise measurement of the contact radius, and of the lubricant film thickness distribution from the interferograms. The correlation between this experimental result and the theoretical deformation of the steel ball allow the bijection between the RGB or HIS color parameters and the nanometer gap between two solids. This technology permit to analyze the thickness of residual water film on the wiping zone, and allows observing the contact area during the wiping phenomenon. The Figure 3 presents an example of the wiping visualization without squealing. The elastomer asperities in contact appear in the contact zone in orange color.

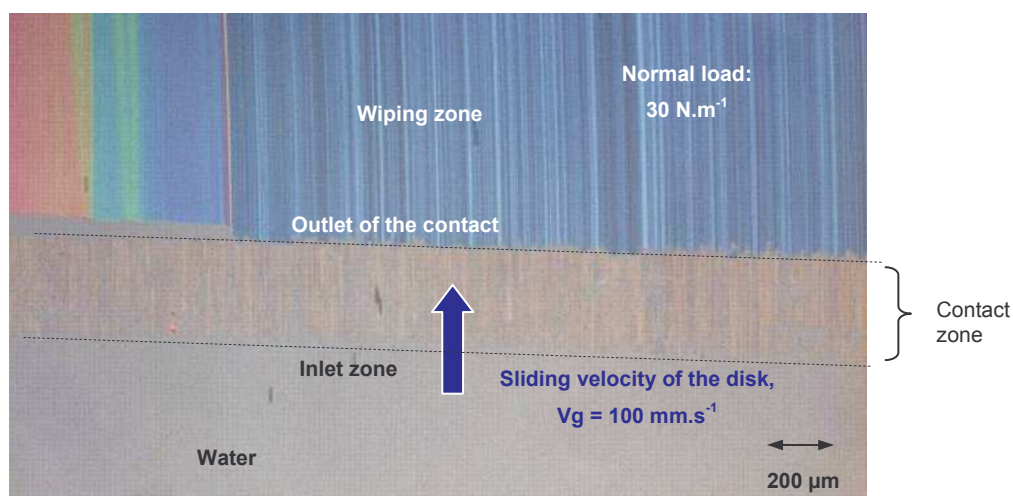


Figure 3: Contact visualization without squealing, water film thickness analysis

This observation permits to analyze the wiping performance. On the top of the image, the dark blue color reveals the dry zone of the disk and the light blue streak reveals small water streaks.

2.4 Experimental methodology

All experiments have been performed in air and at room temperature. The glass surface is cleaned in an ultra sound bath using separate bath of propanol and acetone. They are dried with a nitrogen flow. The elastomer part is decontaminated with the same nitrogen flow.

Different configurations are studied, from dry to wet conditions but this study focuses on the wet one. In fully wet conditions, water is regularly injected in order to maintain the contact supply that is to say the lubricating effect. Sliding velocity and normal load and the lip length are the main parameters of the study.

3 RESULTS AND DISCUSSION

3.1 Squealing phenomenon

Thanks to these measurements, the noise occurrence is a function of the sliding velocity evolution. This correlation is unclear so this paper analyzes the velocity effect.

In first time, the squealing is observed for constant parameters in order to characterize the phenomenon. The experiment was performed at 100 mm.s^{-1} sliding velocity, the normal load is equal to 1N in fully wetting conditions.

The Figure 4 presents the squealing phenomenon of a 0.5 mm radius cylinder/glass configuration. The visualization of the contact shows the same image as previously (Figure 3) but the residual water film on the glass is different. It is noted a fluctuation of this thin water film due to the vibration of the contact edge.

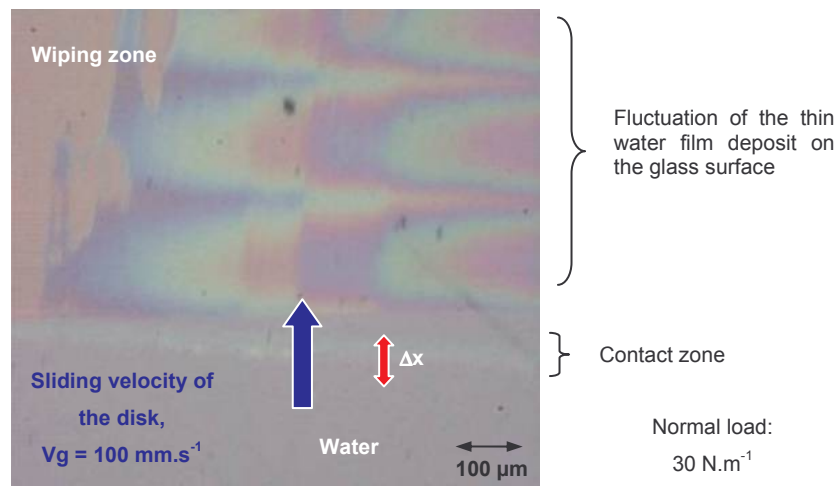


Figure 4: Squealing contact visualization

The contact displacement (Δ_x) and the lip vibration velocity measured by vibrometer technique are presents in the Figure 5. The signals are periodic and the frequency of the fundamental signal is 1038 Hz. It can be deduced that it is stick slip instabilities because when the vibration velocity of the lip reaches the disk sliding velocity ($V_g = 100 \text{ mm.s}^{-1}$), stick phases occur.

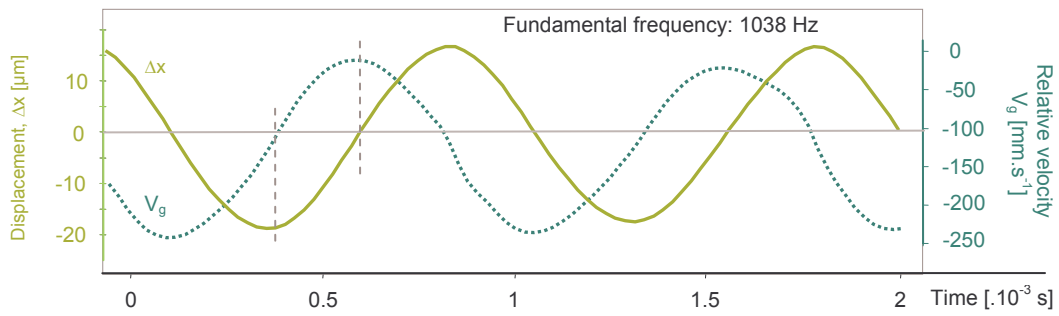


Figure 5: Velocity and displacement vibrations evolution during a squealing phenomenon

The force oscillation is observed in the normal and tangential directions. The friction force (F_x), the normal load (F_N) evolution at the interface have the same periodic shape with the same fundamental frequency (i.e. 1038 Hz). Therefore, the Figure 8 demonstrates that the squealing phenomenon has a tribological origin. The frictional instability creates the contact vibration. The second observation of these signals (Figure 8) is the fluctuation of the friction coefficient during squealing. All simulation take a constant friction coefficient is order to study vibration occurrences. This experimental approach proves that this hypothesis had to be modified.

Thus, the time shift (Δt), between the friction force (F_x) and the normal load (F_N) fluctuations can be related to the rubber viscoelasticity or to the contact stiffness fluctuation by the lip deformation. The tilted angle of the lip controls the level repartition of the force oscillation between the frictional or normal direction.

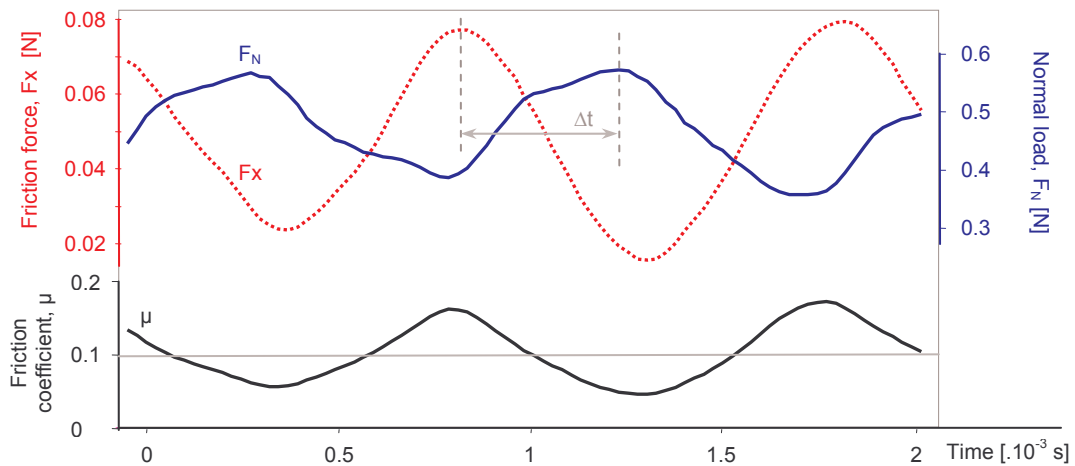


Figure 6: Signal force sensors evolution during a squealing phenomenon

The evolution of the acoustic pressure (Pa) of the sound emission is presents in the Figure 7. The noise emissions are often associated with micrometric contact oscillations, so the friction force instability is at the origin of the noise emission.

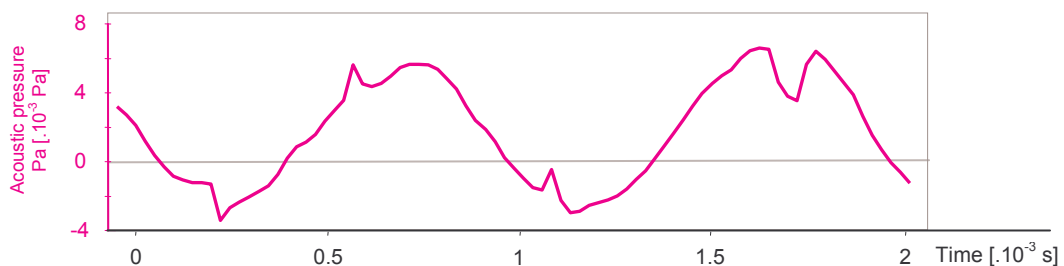


Figure 7: Acoustic pressure evolution during a squealing phenomenon

The second interesting point of this work is that the elastomer sample support is more rigid than the lip stiffness and proves that the vibration is a local aspect. All experiments permit to characterize the level and frequency of vibrations and validate the fact that is the same squealing phenomenon which occurs on automotive. So the vibration finds its origin at the interface so at a local scale and it is not a global structure vibrations.

3.2 Squealing occurrences

In wet condition, the water quantity has no influence on the vibration phenomenon but the vibration stop when the contact is dried.

The impact of the normal load increase is clearly reduced because the frequency remains similar but the vibration level decreases.

If the elastomer/glass couple does not squeal in these previous selected conditions ($V_g = 100 \text{ mm.s}^{-1}$, $F_N = 1 \text{ N}$ in fully wetting conditions), it can be deduced that this contact configuration may not produce noise in all wet conditions.

The main result is that the sliding velocity is the only parameter that controls the vibration generation: below a low critical velocity ($V_{g1} = 10 \text{ mm.s}^{-1}$) and beyond a high critical velocity ($V_{g2} = 150 \text{ mm.s}^{-1}$) the contact is in a steady sliding regime. The squealing systematically appears between these two critical sliding velocities.

In order to explain this result, friction behavior had been characterized. The friction experiments have been performed at 1 N and for sliding velocity ranging from $100 \mu\text{m.s}^{-1}$ to 2 m.s^{-1} in fully wet conditions. The evolution of the friction force versus the sliding velocity is presented in Figure 8 in semi-logarithmic scale for the 0.5mm radius sample geometries.

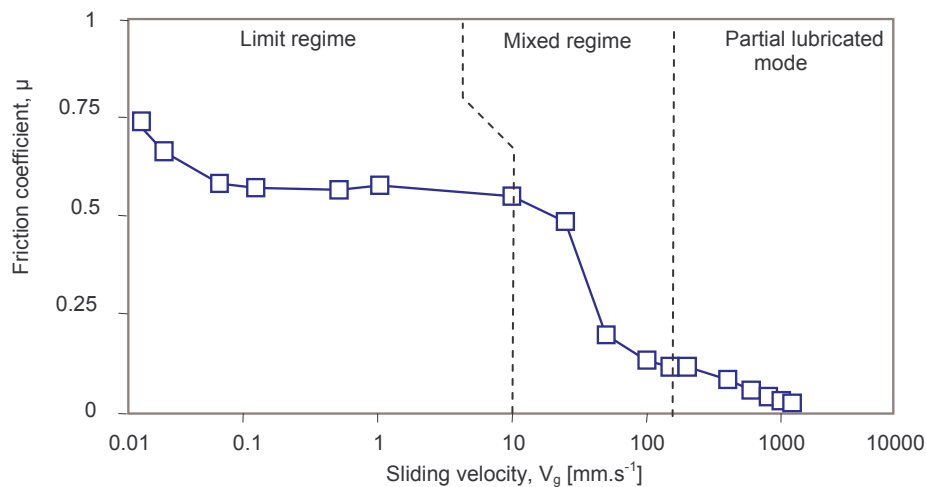


Figure 8: Friction coefficient evolution versus the sliding velocity in wet condition

It can be noted that the evolution versus velocity of the friction force looks like a Stribeck curve [24]. Three different friction regimes can be defined [1]:

- At low sliding velocity ($V_g < 10 \text{ mm.s}^{-1}$), the friction level remains high ($\mu \approx 0.6$). The contact is in the *boundary regime*. The friction force is still governed by the contribution of the dry area.
- Progressively as the velocity increases, a thin film lubrication process is initiated. In the same time, the friction force rapidly decreases: the *mixed regime* appears. The friction force had two contributions: The dry area zone interaction and the lubricated one. This intermediate regime for the studied configuration occurs in the 10 to

150mm.s⁻¹ speed range. This regime is delimited by a low critical velocity ($V_{c1} \approx 10$ mm.s⁻¹), and a high sliding velocity ($V_{c2} \approx 150$ mm.s⁻¹).

- Thus as the speed augments, the contact evolves slowly to a *partially lubricated regime* because a strong reduction of friction is noted ($\mu \approx 0.1$).

The noise emission occurrence appears in the 10-150 mm.s⁻¹ sliding velocity range and corresponds to the mixed regime. In this friction regime the friction force decreases with the velocity increases. This behavior favors the apparition of stick slip vibrations according to Tabor's analysis [12]. In this conditions, the sliding velocity decreases when the adhesive phenomenon appears between the elastomer slider and the glass. The sliding velocity is always reduced because the adhesive aspect augments due to the velocity decrease.

The squealing is always associated to the mixed friction regime so the friction behavior is at the origin of the noise generation problem. To stop vibration, the friction had to be modified.

4 CONCLUSIONS

The first main result of this work is the development of a specific configuration of an ElastoHydroDynamical apparatus in order to reproduce the wiper/glass contact in controlled environment. The original application is the high speed contact visualization with the water film thickness analysis with the simultaneously dynamical measurements (force, displacement, acoustic pressure).

This tribometer allows concluding that the contact vibrations occur only in wet conditions in a mixed regime of lubrication, independently of the normal load. The decreasing behavior of the friction coefficient is at the origin of the noise generation. The frequency of the contact edge displacement and the noise emission and all force signals are at the same frequency and reach 1 kHz. This demonstrates that the friction vibration is at the origin of the squeal noise and the structure stiffness of the sample support does not interfere. Only the lip vibration produces the noise emission. Complementary measurements on car lead the same conclusion.

Other parameters such as the lip length, the vibrating mass are studied in order to find a solution to stop squealing phenomenon on windscreen. The main difficulty is in the friction coefficient control. The squealing problem can not be solving without a tribological analysis.

5 ACKNOWLEDGEMENTS

The authors acknowledge Valeo Research & Development Center (France) for active collaboration and financial support and the French National Research Agency for its project ANR-06-BLAN-0115.

6 REFERENCES

- [1] Deleau F, et al. Sliding friction at elastomer/glass contact: Influence of the wetting conditions and instability analysis. *Tribology International* (2008), doi:10.1016/j.triboint.2008.04.012.
- [2] Schallamach. How does rubber slide? *Wear*, 1971, vol. 17, pp. 301-312.
- [3] Golden J.M. A molecular theory of adhesive rubber friction. *Journal of Physics A: Mathematical and Theoretical*, 1975, vol. 8, no. 6, pp. 966-979.
- [4] Barquins M. Le frottement du caoutchouc et ses instabilités, 16ième Congrès français de mécanique, 2003.
- [5] Bureau L. Élasticité et rhéologie d'une interface macroscopique: du piégeage au frottement solide, Thèse de l'Université Paris VI, 2002.

- [6] Baumberger. Nonlinear analysis of the stick-slip bifurcation in the creep-controlled regime of the dry friction. *Physical review*, 1995, volume 51.
- [7] Ragot P. Contribution à la compréhension robuste en dynamique des systèmes. Thèse Ecole Nationale Supérieure d'Ingénieurs Sud Alsace, 2007.
- [8] Vola D. Friction and instability of steady sliding: squeal of a rubber/glass contact, *Int. J. Numer. Meth. Engng.* 46, 1999, pp. 1699-1720.
- [9] Shinya G. Clarification of the mechanism of wiper blade rubber squeal noise generation, *SAE Japan Review* 22, 2001, pp. 57-62.
- [10] Sinou J.J., Thouverez F., Jezequel L., Mazet G.B., Etude de la stabilité et prédiction des niveaux vibratoires, par modélisation, d'un frein aéronautique, *Proc. Journées Européennes du freinage*, 245-251, 2002.
- [11] Chevennement, Mise en évidence des instabilités d'un système d'essuyage par analyse vibratoire. Corrélation avec un modèle théorique, *Mécanique & Industries*, 341-349, DOI: 10.1051/meca:2006048, 2006.
- [12] Tabor, D., 1955, *Proc. R. Soc. A* 229 198-220.
- [13] Johnson K., Kendall K., and Roberts A. Surface energy and the contact of elastic solids, *Proc. R. Soc. London*, 1971, Ser. A, 324, pp. 301-313.
- [14] Persson B.N.J. On the theory of rubber friction, *Surface Science* 401, 1998, pp. 445-454.
- [15] Bowden F.P. and Tabor D. *The friction and lubrication of solids*, Clarendon Press Oxford, 1986 Baney J., and Hui C. A cohesive zone model for the adhesion of cylinders, 1997, *Journal of Adhesion, Sci. Technol.* 11, pp. 392-406.
- [16] Blouet J., Barquins M. Frottement, Usure et lubrification des élastomères. *Ingénieurs de l'automobile* Novembre décembre 1978, vol. 11-12, pp. 687-706.
- [17] Williams M.L., Landel R.F., and Ferry J.D. *J. Am. Chem. Soc.* 1955.
- [18] Koenen A., Sanon A. Tribological and vibroacoustic behavior of a contact between rubber and glass (application to wiper blade), *Valeo Wiper System*, 2007.
- [19] Roberts A.D. Squeeze film between rubber and glass, *Journal of Physics D: Applied Physics*, 1971, Vol. 4, pp. 423-434.
- [20] Mourrier Louis, Optimisation des contacts ElastoHydroDynamiques par la Micro Texturation de Surface, Application aux systèmes de distribution automobile, Thèse à l'Ecole Centrale de Lyon, 2007.
- [21] Desmond F. Moore, *The friction and lubrication of elastomers*, Pergamon press, 1972, N°77-181328.
- [22] Persson B.N.J. et al. Rubber friction on wet and dry road surfaces : sealing effect. *Physical review B*, 2005.
- [23] Westlake FJ, Cameron A. Optical ElastoHydroDynamic fluid testing, *ASLE Transaction*, 1972, vol. 15, pp. 81-95.
- [24] Begout M., Les problèmes liés au frottement d'élastomère- verre dans l'automobile, université Paul Sabatier Toulouse, Thèse de Doctorat, n° 2206, 1979.